

STABILIZED AND INEXACT ADAPTIVE METHODS FOR CAPTURING INTERNAL LAYERS IN QUASILINEAR PDE

SARA POLLOCK

ABSTRACT. A method is developed within an adaptive framework to solve quasilinear diffusion problems with internal and possibly boundary layers starting from a coarse mesh. The solution process is assumed to start on a mesh where the problem is badly resolved, and approximation properties of the exact problem and its corresponding finite element solution do not hold. A sequence of stabilized and inexact partial solves allow the mesh to be refined to capture internal layers while an approximate solution is built eventually leading to an accurate approximation of both the problem and its solution. The innovations in the current work include a closed form definition for the numerical dissipation and inexact scaling parameters on each mesh refinement, as well as a convergence result for the residual of the discrete problem. Numerical experiments demonstrate the method on a range of problems featuring steep internal layers and high solution dependent frequencies of the diffusion coefficients.

1. INTRODUCTION

This investigation continues the work in [22, 21] developing adaptive numerical methods for quasilinear partial differential equations featuring steep internal layers, in which the solution process starts on a coarse mesh where the problem is not yet resolved. Throughout the coarse mesh and preasymptotic regimes, standard methods such as Newton iterations are known to fail due to both the ill-conditioned and possibly indefinite Jacobians which are characteristic of the approximate discrete problems, and the partial resolution of the problem data. This paper specifies an appropriate set of parameters that may be used in the stabilized σ -Newmark strategy of [21] applied to quasilinear diffusion problems, where the layers develop from both the solution dependent coefficients and a variable dependent source. For the class of problems studied here

$$-\operatorname{div}(\kappa(u)\nabla u) - f(x) = 0, \quad u = 0 \text{ on } \partial\Omega, \quad \text{and} \quad (1.1)$$

$$-\operatorname{div}(\kappa(|\nabla u|^2)\nabla u) - f(x) = 0, \quad u = 0 \text{ on } \partial\Omega, \quad (1.2)$$

in which the diffusion is bounded away from zero, local uniqueness of the solution is known, as well as approximation properties for the finite element solution using linear elements [24], assuming the mesh is sufficiently fine. For operators containing steep solution-dependent layers in the coefficients, the approximation properties of the discrete solution are useful only if the solution to the discrete nonlinear problem can be attained, and the current method attains such a solution by means of a sequence of approximate problems with inexact source functions that limit to the discrete problem.

The methodology is to first discretize (1.1) and (1.2) on each mesh refinement then linearize the resulting discrete problem, and to partially solve the sequence of resulting inaccurate and ill-conditioned coarse mesh problems by stabilized Newton-like iterations

Date: September 24, 2021.

Key words and phrases. Nonlinear diffusion, quasilinear equations, adaptive methods. pseudo-transient continuation, Newton-like methods, inexact methods, regularization .

while adaptively refining the mesh leading to an accurate and efficient solve of an accurate discretization of the problem. In previous work the focus was on the stabilization of the Jacobian by a combination of regularization and added numerical dissipation. Currently, a formula for the numerical dissipation parameter is presented, along with a new inexact method designed for problems where the variable-dependent source dominates the residual of the Newton-like iterations.

Iterative rescaling techniques in the solution of nonlinear problems are not uncommon, see for instance the scaling iterative algorithm (SIA) of [5] for the solution of semilinear elliptic problems, in which the solution u is rescaled at each iteration. The rescaling of the Monge-Ampère equation in [1] to establish a fixed-point argument and recover a numerical solution without having to assume the solution is small enough motivated the current approach. Here, the inexact method rescales the variable dependent source until the solution iterates attain sufficient stability to solve for the given data.

Recent approaches such as [9, 11] for monotone quasilinear problems use inexact linear and nonlinear solves to avoid over-solving for the residual when the Galerkin or discretization error are the dominant sources of error. It is assumed in their analysis that the discrete problem on each refinement is well posed. In the problems studied here, the coarse mesh problem may not be well posed, and may be a sufficiently bad approximation of the exact problem that estimates of the different error sources are not necessarily well determined or useful. Instead, the iterations are ended when they stabilize to the predicted linear convergence rate, which is a function of the numerical dissipation parameter. Combined with the criteria that the residual from the linear solves on each mesh refinement must show sufficient decrease with respect to the residual on the previous refinement, the sequence of stabilized and inexact problems recovers the unscaled discrete problem on a mesh where it is better represented, and with an initial guess for the Newton-like iterations that yields the discrete problem solvable. This method predicts the stability of the solve and allows the sequence of coarse mesh problems to be solved approximately through the preasymptotic regime leading to an efficient solve in the asymptotic regime.

The remainder of the paper is organized as follows. Section 2 states the target problem class and the formulation of the discrete problems. Section 3 reviews the Jacobian stabilization techniques developed by the author in previous work, and which are further developed here. Section 4 presents a formulation for the numerical dissipation parameter γ and characterizes its properties within the adaptive framework; then Section 5 presents a formulation for the inexact scaling parameter δ and characterizes its convergence to unity within the adaptive method. Section 6 summarizes the results of the previous three sections into an adaptive algorithm and proves the convergence of the residual of the discrete problem. Finally, Section 7 demonstrates the method with a collection of numerical experiments featuring different types of internal layers.

The following notation is used throughout the rest of the paper. In defining the weak and bilinear forms in the next section $(u(x), v(x)) = \int_{\Omega} u(x)v(x) dx$, and in later section the discrete inner product between vectors $u_k, v_k \in \mathbb{R}^n$ is denoted $\langle u_k, v_k \rangle$. The norm $\|\cdot\|$ where not otherwise specified is the L_2 norm. The n th iterate subordinate to the k th partition \mathcal{T}_k is denoted u_k^n , while u^n is the n th iteration on a fixed partition and u_k is the final iteration on the k th mesh, taken as the approximate solution on \mathcal{T}_k .

2. TARGET PROBLEM CLASS

The class of problems considered are quasilinear diffusion problems $F(u, x) = 0$, over polygonal domain $\Omega \subset \mathbb{R}^2$, with $F : X \times \Omega \rightarrow Y^*$ and $F'(u, x) := F_u(u, x) \in \mathcal{L}(X, Y^*)$,

where $F(u, x)$ is given by

$$F(u, x) := -\operatorname{div}(\kappa(u)\nabla u) - f(x) = 0, \text{ in } \Omega \in \mathbb{R}^2, \quad u = 0 \text{ on } \partial\Omega, \text{ or} \quad (2.1)$$

$$F(u, x) := -\operatorname{div}(\kappa(|\nabla u|^2)\nabla u) - f(x) = 0, \text{ in } \Omega \in \mathbb{R}^2, \quad u = 0 \text{ on } \partial\Omega, \quad (2.2)$$

with $f(x) \in L_2(\Omega) \cap L_\infty(\Omega)$. Multiplication against test functions $v \in Y$ and integration by parts yields the weak form of each problem

$$B(u, v) = (\kappa(u)\nabla u, \nabla v) = (f, v), \quad \text{for all } v \in Y, \quad \text{for (2.1),} \quad (2.3)$$

$$B(u, v) = (\kappa(|\nabla u|^2)\nabla u, \nabla v) = (f, v) \quad \text{for all } v \in Y, \quad \text{for (2.2).} \quad (2.4)$$

The linearized form induced by $F'(u, x) := F_u(u, x)$, is determined by taking the Gateaux derivative in direction $w \in X$ by $B'(u; w, v) = \lim_{t \rightarrow 0} d/dt (B(u + tw, v))$ yielding

$$B'(u; w, v) = (\kappa(u)\nabla w, \nabla v) + (\kappa'(u)w\nabla u, \nabla v), \quad \text{for (2.1),} \quad (2.5)$$

$$B'(u; w, v) = (\kappa(|\nabla u|^2)\nabla w, \nabla v) + (\kappa'(|\nabla u|^2)(2\nabla u \cdot \nabla w)\nabla u, \nabla v), \quad \text{for (2.2).} \quad (2.6)$$

Both types of problems fit into the context of [24] with the assumption that there is a solution $u \in H_0^1(\Omega) \cap W_{2+\varepsilon}^2(\Omega)$ and $F_u(u, x) : H_0^1(\Omega) \rightarrow H^{-1}(\Omega)$ is an isomorphism, in which case the solution u is an isolated solution, and approximation properties for the linear Lagrange finite element solution can be shown to hold, assuming the meshsize is fine enough.

It is further shown in [4] for problems of the form (2.1), assuming $\kappa(s) \geq k > 0$ for all $s \in \mathbb{R}$ and $\kappa(s), \kappa'(s), \kappa''(s)$ bounded, then there exists a unique solution $u \in W^{1,p}(\Omega)$, with $2 < p < \infty$. Moreover, by the analysis of [16], an adaptive method using linear Lagrange finite elements can be shown to converge, again assuming the meshsize is sufficiently small.

The second class of equations (2.2) is considered in for instance [14, 3, 9] and the reference therein, and uniqueness of solutions as well as convergence of adaptive methods have been established supposing a Lipchitz condition and a monotonicity condition such as $B(v, v - w) - B(w, v - w) \geq 0$ or the strong monotonicity condition $B(v, v - w) - B(w, v - w) \geq c\|v - w\|_Y^2$ as in [14], and assuming the approximate discrete problems are well posed.

2.1. Discrete formulation. The discrete problem is, find $u_h \in X_h$ such that $B(u_h, v) = 0$ for all $v \in Y_h$ where $X_h \subset X$ and $Y_h \subset Y$ are discrete spaces of the same finite dimension. Here, X_h and Y_h are finite element spaces with respect to triangulation \mathcal{T}_h , where the family of triangulations $\{\mathcal{T}_h\}_{0 < h < 1}$ is regular and quasi-uniform in the sense of [7]. For the rest of the discussion it is assumed the trial and test spaces are the same: $X = Y$ and $X_h = Y_h$. On each refinement k , the test/trial space X_{h_k} is taken as the linear finite element space V_k consisting of Lagrange finite elements \mathbb{P}_1 over partition \mathcal{T}_k that satisfy the homogeneous Dirichlet boundary conditions.

The resulting discrete problem on refinement k is of the form $G_k(u, x) = 0$ for $u \in V_k$ and $x \in \Omega \subset \mathbb{R}^2$. The decomposition $G_k(u, x) = -g(u) + f_k(x)$ is used throughout the remainder of the discussion. On a given discretization that is not sufficiently fine, $f_k(x)$ may be a bad representation of the given source $f(x)$. On such a coarse mesh, solving the discretized equation $g(u_k) = f_k(x)$ may produce a solution u_k which is a highly inaccurate solution to (2.3), or respectively (2.4), so seeking an exact solution to the approximate problem is not a good use of computational effort.

Ideally, the adaptive method starts on a coarse mesh where the problem is small, if badly resolved. It produces a sequence of approximations that are good enough to refine the mesh to resolve the data and solution dependent coefficients, and upon sufficient resolution and stability, provide a good approximation for the solution to the discrete problem.

The features of the current method as introduced in [22, 21] include an adaptive approach to regularization used to stabilize the Jacobian in the coarse mesh and preasymptotic regimes, also conceived of as adaptively regulated implicit pseudo-time stepping.

3. STABILIZED ADAPTIVE METHOD

The stabilized iterations are designed to fit into the framework of a standard adaptive method, which uses error indicators to mark and refine the mesh. The theoretical results of this paper are independent of the specifics of the adaptive method, and a different set of error indicators could be used. The method here is demonstrated using standard residual based estimators, as in [12, 23] for mesh refinement, and similarly for the adaptive regularization strategy. Both the interior and the jump part of the residual indicator are used to refine the mesh, and a similar jump indicator based only on the solution is used to determine the regularization. The indicators are defined with respect to the consistent problem with unscaled data.

3.1. Adaptive mesh refinement. The local *a posteriori* residual-based indicator, and corresponding jump-based indicator for element $T \in \mathcal{T}_k$ with h_T the element diameter are given by

$$\zeta_T^2(v) = \zeta_{\mathcal{T}_k}^2(v, T) := h_T \|J_T(v)\|_{L_2(\partial T)}^2, \quad (3.1)$$

$$\eta_T^2(v) = \eta_{\mathcal{T}_k}^2(v, T) := h_T^2 \|F(v, x)\|_{L_2(T)}^2 + \zeta_T^2(v), \quad (3.2)$$

$J_T(v) := \llbracket [\kappa(v) \nabla v \cdot n] \rrbracket_{\partial T}$, for problem (2.1) and $J_T(v) := \llbracket [\kappa(|\nabla v|^2) \nabla v \cdot n] \rrbracket_{\partial T}$, for problem (2.2), with jump $\llbracket \phi \rrbracket_{\partial T} := \lim_{t \rightarrow 0} \phi(x + tn) - \phi(x - tn)$, where n is the appropriate outward normal defined on ∂T . The error estimator on partition \mathcal{T}_k is given by the l_2 sum of indicators $\eta_{\mathcal{T}_k}^2 = \sum_{T \in \mathcal{T}_k} \eta_T^2$, and similarly for $\zeta_{\mathcal{T}_k}$.

In these results, the Dörfler marking strategy is used. Given a parameter $\theta \in (0, 1)$ a set of least, or nearly least cardinality is chosen for the marked set \mathcal{M} so the sum of their indicators is greater than the given fraction of the sum of all the indicators.

$$\sum_{T \in \mathcal{M}} \eta_T^2 \geq \theta \sum_{T \in \mathcal{T}_k} \eta_T^2. \quad (3.3)$$

Remark 3.1. *In contrast to an earlier version of the method for convection diffusion problems in [21], no additional coarse mesh marking is performed. Scaling down the variable dependent source on the initial solves allows the method to traverse the preasymptotic and coarse mesh regimes while minimizing refinement that negatively impacts the efficiency of the method in the asymptotic regime.*

3.2. Adaptive regularization. The motivation from multiple perspectives behind the adaptive regularization technique from is described in [22], and an updated strategy is suggested in [21], which is summarized below. The coarse mesh problems may have indefinite, and often have highly ill-conditioned Jacobians, and the Laplacian-based regularization helps make the Newton-like iterations solvable. The adaptive element is introduced to yield faster convergence as the degrees of freedom for which the approximate solution is smooth experience little benefit from the added stabilization as compared to the degrees of freedom (dofs) in regions where the jump in the normal derivative between

neighboring elements is large. On each mesh partition \mathcal{T}_k the penalty matrix $R = R_k$ is a localized version of the Laplacian stiffness matrix denoted R^{global} . First define the jump indicator used to select elements for regularization, c.f., (3.1).

$$\xi_T^2(v) = h_T \| [\nabla v \cdot n] \|_{L_2(\partial T)}^2. \quad (3.4)$$

Using the jump indicators $\{\xi_T\}_{T \in \mathcal{T}}$, select degrees of freedom for regularization.

Definition 3.2. Define R^{global} as the Laplacian stiffness matrix on refinement k . Let D^{loc} a diagonal matrix of zeros and ones, v_j a vertex subordinate to partition \mathcal{T}_k , and $\xi_T = \xi_T(u_k^0)$. Then set

$$\tilde{\psi}_k = \sqrt{\text{median}_{T \in \mathcal{T}_k}(\xi_T^2)}, \text{ and } \psi_k = \begin{cases} \tilde{\psi}_k^{1/2}, & \text{if } \tilde{\psi}_k > 1, \\ \tilde{\psi}_k, & \text{otherwise,} \end{cases}$$

and

$$D_{jj}^{loc} = \begin{cases} 0, & \text{if } \xi_T \leq \psi_k \text{ for each element that contains } v_j \text{ as a vertex,} \\ 1, & \text{otherwise.} \end{cases} \quad (3.5)$$

Set $R_k = D^{loc} R^{global} D^{loc}$.

The regularization matrix R_k defined by Definition 3.2 is positive semidefinite and targeted to smooth regions of high curvature.

3.3. Exact and inexact σ -Newmark iterations. The σ -Newark iteration of [21] generalizes the pseudo-transient continuation method of [18, 8, 13] and similarly the “s” method of [2] to an adaptive framework, combining stabilization by pseudo-time with the Tikhonov-type regularization as used in ill-posed problems [10].

The Jacobian is stabilized by seeking a steady-state solution of the given nonlinear problem $G_k(u, x) = 0$ by solving $\partial(Ru)/\partial t + G_k(u, x) = 0$, and discretizing the time derivative $\dot{u} := \partial u / \partial t$ by a Newmark update [20] given by the time discretization $u^{n+1} = u^n + \Delta t^n \{\gamma \dot{u}^{n+1} + (1 - \gamma) \dot{u}^n\}$, or solving for \dot{u}^{n+1}

$$\dot{u}^{n+1} = \frac{u^{n+1} - u^n}{\gamma \Delta t^n} - \frac{(1 - \gamma)}{\gamma} \dot{u}^n.$$

In the current notation the regularization parameter $\alpha^n = 1/\Delta t^n$. As discussed in the literature on the finite element analysis of structures, for instance [15, 6] and the references therein, the update yields second-order accuracy in time for $\gamma = 1/2$ and increased numerical dissipation of the high frequency modes with $\gamma > 1/2$. The current adaptive method allows $\gamma > 1$, which can be seen to damp the influence of the right-hand side residual. In [21] a secondary linearization is performed to further stabilize the approximate Jacobian resulting in the iteration

$$(\alpha^n R + \gamma^n \{\sigma^n G'(u^n) + (1 - \sigma^n) G'(\bar{u})\}) w^n = -G(u^n, x), \quad u^{n+1} = u^n + w^n. \quad (3.6)$$

In previous discussions the variable dependence of $G(u, x)$ was suppressed and written $G(u)$. In the current presentation the variable dependent load will be stated explicitly by $G(u, x) = g(u) - f(x)$. As the Jacobian $G_u(u, x) = g'(u)$ is invariant to $f(x)$, the stabilization based on the Jacobian alone does not address sharp spikes or steep gradient which may be present in $f(x)$, particularly in partially resolved coarse mesh problems. The inexact iteration is then introduced

$$(\alpha^n R + \gamma^n \{\sigma^n g'(u^n) + (1 - \sigma^n) g'(\bar{u})\}) w^n = -g(u^n) + \delta f(x), \quad u^{n+1} = u^n + w^n. \quad (3.7)$$

Iteration (3.6) is defined by the following parameters on iteration n of refinement k . The limiting behaviors necessary to reduce the stabilized iteration to the standard Newton iteration $g'(u)w^n = -g(u^n) + f(x)$ are noted.

- Regularization parameter $\alpha = \alpha_k^n \geq 0$, $\alpha \rightarrow 0$.
- Semidefinite regularization term $R = R_k$.
- Newmark parameter $\gamma = \gamma_k^n \geq 1$, $\gamma_k^n \rightarrow 1$.
- Stabilization parameter $\sigma = \sigma_k^n \in [\sigma_0, 1]$, $\sigma \rightarrow 1$.

In addition, iteration (3.7) depends on the scaling parameter

$$\delta = \delta_k \leq 1, \delta \rightarrow 1.$$

The focus of this paper is the description of an appropriate choice of parameters γ and δ to use in iterations (3.6) and (3.7). The regularization parameters α and R are presented in [21], and recalled in this section. The convergence behavior of iteration (3.6) is analyzed in [21], and those results are recalled below. Definitions of γ and δ are introduced in the following sections, as well as a convergence result for the sequence of inexact iterations using (3.7).

The following concepts are used throughout the discussion. On a fixed refinement k , the subscript k is removed where it will not cause confusion, *e.g.*, the discretized variable-dependent source f_k is denoted f . The solution dependent part of the residual $g(u^n)$ is denoted g^n , and residual r^n is given by

$$r^n = -g^n + \delta f, \quad (3.8)$$

where $\delta = 1$ for iteration (3.6).

Before introducing the definitions of the numerical dissipation parameter γ and the scaling parameter δ , local convergence the σ -Newmark iteration (3.6) is recalled from [21]. As the scaling parameter δ is held constant over iterations on a given refinement, Theorem 3.6 holds also for the inexact iteration (3.7), where in the first case the residual which converges to zero is given by $r(u, x) = -g(u) + f(x)$ and in the second it is given by $r(u, x) = -g(u) + \delta f(x)$. The proof of local convergence depends on the nonlinear discrete problem, which coincides up to sign with the residual function on a fixed refinement, satisfying a local Lipschitz condition on the Jacobian with respect to u in the vicinity of the exact solution u^* . For simplicity of notation, consider the convergence of $-r(u, x)$ to zero, whose Jacobian is then $g'(u)$. Denote the open neighborhood about u by $N(u, \varepsilon) = \{v \mid \|u - v\| < \varepsilon\}$.

Assumption 3.3. *There exist $\omega_L, \varepsilon > 0$ so that for all $w, v \in N(u^*, \varepsilon)$*

$$\|g'(w) - g'(v)\| \leq \omega_L \|w - v\| \text{ for all } w, v \in N(u^*, \varepsilon).$$

The second set of assumptions addresses the nonsingularity, boundedness and stability of the approximate Jacobian. Assumption 3.5 requires a regularization parameter $\alpha^n < \alpha_M$ for some fixed α_M , which follows from the definition of α^n described in [22], and repeated here for convenience. In accordance with the local convergence Theorem 3.6 the update assures $\alpha^n \leq \|r^n\|$, so long as the residual is decreasing.

Definition 3.4 (Regularization parameter α). *Set $\beta^0 = 1$. For $n \geq 1$,*

$$\alpha^n = \beta^n \|r^n\|, \text{ with}$$

$$\beta^n = \begin{cases} \min\{1, \max\{\beta^{n-1}/2, \|r^n\|/\|r^{n-1}\|\}\}, & \text{if } \|r^n\| < \|r^{n-1}\|, \\ \beta^{n-1}, & \text{otherwise.} \end{cases}$$

The factor β^n of Definition 3.4 modifies α^n to reduce the regularization faster if the residual is decreasing steadily, without inducing rapid fluctuations in the regularization between iterations. So long as the residual is decreasing, $\alpha^n \leq \|r^n\|$ should be maintained to satisfy the hypotheses of the local convergence Theorem 3.6. The last set of assumptions for the local convergence theorem addresses the invertibility and stability of the approximate Jacobian.

Assumption 3.5. *There exist $\beta > 0$ so that for $0 < \sigma_0 \leq \sigma \leq 1$, fixed \bar{u} , positive semidefinite R , $\gamma > 1$, and for all $0 < \alpha_n < \alpha_M$, then for all $u \in N(u^*, \varepsilon)$:*

- 1) $\alpha_n R + \gamma\{(1 - \sigma)g'(\bar{u}) - \sigma g'(u)\}$ is invertible.
- 2) $\|(\alpha_n R + \gamma\{(1 - \sigma)g'(\bar{u}) - \sigma g'(u)\})^{-1}\| \leq M_\gamma \sigma$.
- 3) $\|(\alpha_n R)(\alpha_n R + \gamma\{1 - \sigma\}g'(\bar{u}) - \sigma g'(u))^{-1}\| \leq \frac{1}{1 + \beta\gamma/\alpha_n}$.

The local convergence theorem demonstrates that for a sufficiently small residual, if the incoming iterate u^n is within the basin of attraction of the exact solution u^* , then u^n is also within the basin of attraction, and the residual decreases asymptotically at the rate $\|r^{n+1}\| \leq (1 - 1/\gamma)\|r^n\|$, for $\gamma > 1$.

Theorem 3.6. *Let $\alpha_n \leq \|r(u^n)\| \leq \alpha_M$ and let Assumptions 3.3 and 3.5 hold, and α^n given by Definition 3.4. Define σ by*

$$\sigma = \max \left\{ \sigma_0, 1 - \frac{\|r^n\|}{K_0} \right\}, \quad (3.9)$$

for a given K_0 . Then there exists $\bar{d} > 0$ such that for u^n in the open set \mathcal{S} given by

$$\mathcal{S} = \left\{ u \in N(u^*, \varepsilon) \mid \|r(u)\| < \bar{d} \right\}, \quad (3.10)$$

and u^{n+1} defined by iteration (3.6), or respectively by (3.7) with $\gamma > 1$, it holds that $u^{n+1} \in \mathcal{S}$, and the sequence of residuals converges q -linearly to zero with asymptotic rate $q = 1 - 1/\gamma$.

The proof of Theorem 3.6 is given in [21].

4. UPDATE OF NUMERICAL DISSIPATION.

The numerical dissipation parameter $\gamma \geq 1$ of iterations (3.6) and (3.7) should start large enough to provide sufficient stability to the iterations and decrease down to one in order to recover the quadratic convergence rate of the Newton-like iterations. The parameter is adjusted during the course of iterations on a given refinement whenever the observed rate of convergence is within tolerance of the expected rate, $(1 - 1/\gamma)$. In order to ensure a decrease in γ as it is updated, each γ_k^n must be bounded by an appropriate γ_{MAX} , with respect to the user set rate tolerance, ε_T .

Assumption 4.1. *Given a rate tolerance ε_T , γ_k^n is bounded above for all n, k by γ_{MAX} , satisfying*

$$\gamma_k^n \leq \gamma_{\text{MAX}} < 1/\varepsilon_T. \quad (4.1)$$

This assumption has been observed to be necessary, and γ can indeed grow without bound if allowed greater than $1/\varepsilon_T$. It is also of practical value not to set the rate tolerance ε_T too low, as the update of γ can stall for some number of refinements due to the partial capturing of the solution and variable dependent layers in the preasymptotic regime. In the examples presented in Section 7, ε_T is chosen either as 0.005 or 0.01, where the larger value is chosen in the case where steep gradients prevent the resolution of the

Jacobian, and this adjustment is sufficient to speed the update of γ without compromising stability of the method. With these parameters, the update of γ on a given refinement k is performed when the following criteria are met.

Criteria 4.2 (γ update). *Given a user set tolerance ε_T , and $\gamma^n < \gamma_{\text{MAX}}$ satisfying Assumption 4.1, and a minimum number of iterations between updates I_{\min} , the dissipation parameter γ^n is updated after each iteration n on which all the following criteria hold.*

1) $\gamma^n > 1$.

2) *The observed rate of convergence is within tolerance of the predicted value*

$$\left| \frac{\|r^{n+1}\|}{\|r^n\|} - \left(1 - \frac{1}{\gamma^n}\right) \right| < \varepsilon_T. \quad (4.2)$$

3) *The observed rate of convergence is sufficiently stable.*

$$\left| \frac{\|r^{n+1}\|}{\|r^n\|} - \frac{\|r^n\|}{\|r^{n-1}\|} \right| < \varepsilon_T. \quad (4.3)$$

4) *At least $I_{\min} \geq 2$ iterations have passed since the last update of γ .*

The last condition of Criteria 4.2 is necessary to assure the three consecutive residuals of (4.3) are computed with the same value of γ , and show the requisite rate stability. Given a reduction factor $q = q_\gamma < 1$, on satisfaction of Criteria 4.2 after iteration n of fixed refinement k , γ^{n+1} is updated as follows.

Definition 4.3. *Given an initial $\delta_0 > 1$, for $k > 0$*

$$\tilde{\gamma}^{n+1} = q \cdot \frac{\langle r^n, r^n \rangle}{\langle r^n, g^{n+1} - g^n \rangle}, \quad \gamma^{n+1} = \max \{1, \tilde{\gamma}^{n+1}\}. \quad (4.4)$$

To see this update is reasonable as the algorithm attains convergence, observe the ideal value of g^{n+1} is δf , implying $r^{n+1} = 0$, and the ideal value of $g^{n+1} - g^n$ is $\delta f - g^n = r^n$, so that $\gamma^{n+1} = 1$, if the iteration produces a zero residual. Based on condition (4.2) of Assumption 4.2, the updated quantity γ^{n+1} is bounded above and below in terms of γ^n , and is then shown to be decreasing, on the condition of Assumption 4.6. Lemma 4.4 bounds the denominator $\langle r^n, g^{n+1} - g^n \rangle$, then Corollary 4.5 bounds the ratio determining γ^{n+1} .

Lemma 4.4. *Under (4.2) of Assumption 4.2, with tolerance ε_T the following upper and lower bounds hold.*

$$\|r^n\|^2 \left(\frac{1}{\gamma^n} - \varepsilon_T \right) < \langle r^n, g^{n+1} - g^n \rangle < \|r^n\|^2 \left(2 - \frac{1}{\gamma^n} + \varepsilon_T \right). \quad (4.5)$$

Proof. Rewriting g^n and g^{n+1} in terms of the residual

$$\langle r^n, g^{n+1} - g^n \rangle = \langle r^n, -g^n + \delta f - (-g^{n+1} + \delta f) \rangle = \langle r^n, r^n - r^{n+1} \rangle. \quad (4.6)$$

For the first inequality

$$\langle r^n, r^n \rangle - \langle r^n, r^{n+1} \rangle \geq \|r^n\|^2 - \|r^n\| \|r^{n+1}\| = \|r^n\|^2 \left(1 - \frac{\|r^{n+1}\|}{\|r^n\|} \right). \quad (4.7)$$

Bounding the ratio of residuals on the right by (4.2)

$$1 - \frac{\|r^{n+1}\|}{\|r^n\|} > \frac{1}{\gamma^n} - \varepsilon_T. \quad (4.8)$$

Applying (4.7) and (4.8) to (4.6), the result follows.

For the second inequality of (4.5), applying Cauchy-Schwarz and triangle inequalities to (4.6)

$$\langle r^n, r^n - r^{n+1} \rangle \leq \|r^n\| \|r^n - r^{n+1}\| \leq \|r^n\|^2 + \|r^n\| \|r^{n+1}\|. \quad (4.9)$$

By (4.2), $\|r^{n+1}\| < \|r^n\|(1 - 1/\gamma + \varepsilon_T)$, from which the result follows. \square

The upper and lower bounds on $\tilde{\gamma}^{n+1}$ now follow from (4.5).

Corollary 4.5. *Under Assumption 4.1 and Criteria 4.2, the update of γ^n to $\tilde{\gamma}^{n+1}$ of (4.4) satisfies the following bounds.*

$$\frac{q \cdot \gamma^n}{\gamma^n(2 + \varepsilon_T) - 1} < \tilde{\gamma}^{n+1} < \frac{q \cdot \gamma^n}{1 - \varepsilon_T \gamma^n}. \quad (4.10)$$

Proof. The argument follows from direct application of Lemma 4.4 to the definition of $\tilde{\gamma}^{n+1}$ given by (4.4). The upper bound

$$\tilde{\gamma}^{n+1} = q \cdot \frac{\|r^n\|^2}{\langle r^n, g^{n+1} - g^n \rangle} < q \cdot \frac{1}{1/\gamma^n - \varepsilon_T} = \frac{q \cdot \gamma^n}{1 - \varepsilon_T \gamma^n},$$

holds under Assumption 4.1, which assures the positivity of the denominator. Similarly, the lower bound follows applying $\gamma > 1$, the first condition of update Criteria 4.2. \square

The lower bound remains satisfied in the case $\gamma^{n+1} = 1$ by Definition 4.3, and the upper bound is of no interest as the goal of the sequence is to decrease γ to unity in a stable manner. To establish the monotonic decrease of γ , and more generally the decrease at rate $1 > \bar{q} > q$, the following Assumption 4.6 strengthens the Assumption 4.1, used to establish the upper bound of (4.10).

Assumption 4.6 (Monotone decrease of γ). *Given a reduction factor q , a rate of decrease $\bar{q} > q$, and rate tolerance ε_T , let γ_k^n be bounded above for all n, k by γ_{MONO} satisfying*

$$\gamma_k^n \leq \gamma_{\text{MONO}} = \frac{1}{\varepsilon_T} \left(1 - \frac{q}{\bar{q}} \right). \quad (4.11)$$

In practice, setting $\bar{q} = 1$ and $\gamma < (1 - q)/\varepsilon_T$ ensures γ will be nonincreasing, although for more stability in the earlier iterations, the weaker condition $\gamma < \gamma_{\text{MAX}}$ is sufficient, and after γ reduces below γ_{MONO} the monotonicity holds.

Corollary 4.7 (Monotonic decrease of γ). *For γ^{n+1} determined by (4.4) on the satisfaction of Criteria 4.2, and Assumption 4.6 with $\bar{q} = 1$, the sequence $\{\gamma^n\}_{n \geq 0}$ is nonincreasing. Moreover, assuming (4.11) with $1 < \bar{q} < q$, then for $\gamma^{n+1} = \tilde{\gamma}^{n+1} > 1$, the sequence satisfies $\gamma^{n+1} < \bar{q}\gamma^n$.*

The proof follows from the upper bound on $\tilde{\gamma}^{n+1}$, given by (4.10) of Corollary 4.5.

Proof. To assure $\tilde{\gamma}^{n+1} \leq q\gamma^n/(1 - \varepsilon_T \gamma^n) < \bar{q}\gamma^n$, require

$$q < \bar{q}(1 - \varepsilon_T \gamma^n), \quad (4.12)$$

which is satisfied by Assumption 4.6. To establish the monotonic decrease without a rate, set $\bar{q} = 1$ in (4.12), and rearrange terms to obtain $\gamma^n < (1 - q)/\varepsilon_T$ as the necessary condition. \square

While the determination of the monotonic decrease of γ with a given rate \bar{q} to unity follows in a straightforward manner from Definition 4.3, condition (4.2), and Assumption 4.6, this establishes the important property that if the algorithm does not reset after a given point, $\gamma^N = 1$ will be achieved after at most $N - n = \lceil -\log(\gamma^n)/\log(\bar{q}) \rceil$ updates, where $\lceil \cdot \rceil$ denotes the ceiling function. Notably, $N - n$ counts only the updates

of γ , independent of the number of mesh refinements that occur over the course of those updates. The more delicate point of whether those updates occur, which requires the predicted convergence rate is achieved within tolerance, is addressed in Theorem 6.6, which relies on Theorem 3.6, the local convergence with rate of iterations (3.6) and (3.7).

5. UPDATE OF SCALING PARAMETER

The scaling parameter δ for the inexact iteration (3.7) is computed on the completion of the iterations for refinement k . This is in contrast to the update on γ , performed whenever the iterations converge close enough to the predicted rate. This strategy is reasonable as updating δ changes the discrete problem which already changes on each refinement. Except for the first, the criteria to update δ are a subset of the conditions used to exit the Newton-like iterations on each refinement. The last two conditions of Criteria 5.1 are closely related to (4.2) and (4.3), the second and third conditions of Criteria 4.2, the update on γ . The acceptable rate criterium (5.2) is weaker than the requirement (4.2), and the stability criterium (5.3) requires the observed rate has not decreased by much compared to the previous observed rate. Distinct from the conditions to update γ , the second condition of Criteria 5.1 requires the current and previous residual to be smaller than the initial residual of the current refinement and final residual of the previous refinement. This condition is important to ensure the algorithm convergences, and the sequence of residuals r_k decrease at a rate

$$\|r_k\| < \|r_{k-1}\|(1 - 1/(2\gamma_k^n)) \leq \|r_{k-1}\|(1 - 1/(2\gamma_{\text{MAX}})),$$

on Assumption 4.1, or

$$\|r_k\| < \|r_{k-1}\|(1 - 1/(2\gamma_k^n)) \leq \|r_{k-1}\|(1 - 1/(2\gamma_{\text{MONO}})),$$

on Assumption 4.6, where r_k is the final residual on refinement k . Conditions (5.2) and (5.3) are also important to the stability of the update, and assure $g^{n+1} = g(u^n + w^n)$ has been improved by two consecutive steps w^{n-1} and w^n .

Criteria 5.1 (δ update). *Given a user set rate tolerance ε_T as in Criteria 4.2 and a convergence tolerance ε_{CON} , the iterations are terminated and δ is updated after iteration n of refinement k , when conditions (1-4) are all met, or when conditions (1) and (5) are satisfied.*

1) $\delta_k < 1$. If $\delta_k = 1$, it is not updated.

2) Sufficient decrease in the sequence of residuals $\|r_k\|$

$$\|r_k^n\| < \min\{\|r_k^0\|, \|r_{k-1}\|\}. \quad (5.1)$$

3) The observed rate of convergence is beneath the accepted rate $(1 - 1/2\gamma)$

$$\frac{\|r^{n+1}\|}{\|r^n\|} < 1 - \frac{1}{2\gamma^n}. \quad (5.2)$$

4) The observed rate is sufficiently stable

$$\frac{\|r^{n+1}\|}{\|r^n\|} + \frac{\varepsilon_T}{2} > \frac{\|r^n\|}{\|r^{n-1}\|}. \quad (5.3)$$

5) $\|r^n\| < \varepsilon_{\text{CON}}$. The iteration reached convergence.

On satisfaction of Criteria 5.1, δ is updated based on replacing the satisfied linearized equation

$$\{\alpha^n R_k + \gamma^n (\sigma^n g'(u^n) + (1 - \sigma^n) g'(\bar{u}))\} w^n = -g^n + \delta_k f_k, \quad (5.4)$$

with the corresponding relation found by replacing $g'(u^n)w^n$, with $g^{n+1} - g^n$, modifying the right hand side residual by $q < 1$ to obtain

$$\{\alpha^n R_k + \gamma^n ((1 - \sigma^n)g'(\bar{u}))\}w^n + \gamma^n \sigma^n (g^{n+1} - g^n) = -g^n + q\delta_{k+1}f_k, \quad (5.5)$$

and considering the discrete inner product of both sides against the source $f = f_k(x)$. Given a factor $q = q_\delta < 1$, at the end of each nonlinear solve, δ_{k+1} is determined by

$$\langle f, \{\alpha^n R_k + \gamma^n ((1 - \sigma^n)g'(\bar{u}))\}w^n + \gamma^n \sigma^n (g^{n+1} - g^n) \rangle = \langle f, -g^n + q_k \delta_{k+1} f \rangle, \quad (5.6)$$

resulting in the following definition.

Definition 5.2. Given an initial $\delta_0 < 1$, for $k > 0$

$$\tilde{\delta}_{k+1} = \frac{\langle f, \gamma \sigma (g^{n+1} - g^n) + (\gamma(1 - \sigma)g'(\bar{u}) + \alpha R)w^n + g^n \rangle}{q_k \|f\|^2}, \quad (5.7)$$

$$\delta_{k+1} = \min\{1, \tilde{\delta}_{k+1}\}, \quad (5.8)$$

with $R = R_k$, $\alpha = \alpha^n$, $\gamma = \gamma^n$ and $\sigma = \sigma^n$.

The sequence for $\delta_k < 1$ can also be expressed recursively by considering (5.4), satisfied exactly with $\delta = \delta_k$, and subtracting the corresponding inner product against f from (5.6). Expressed in terms of the one-step linearization error $\mathcal{L}^e(u^n)$ given by

$$\mathcal{L}^e(u^n) := g^{n+1} - g^n - g'(u^n)w^n, \quad g^{n+1} = g(u^n + w^n), \quad (5.9)$$

the recursive relation for δ may be written

$$\delta_{k+1} = \frac{1}{q_k} \left\{ \delta_k + \frac{\gamma \sigma}{\|f\|^2} \langle f, \mathcal{L}^e(u^n) \rangle \right\}. \quad (5.10)$$

From (5.10), the local Lipschitz Assumption 3.3 on $g'(u_k^n)$ is used to show the convergence of δ to one as the residual attains convergence. First, a bound on δ_{k+1} with respect to δ_k is established.

Lemma 5.3. Assume $u_k^n \in N(u_k^*, \varepsilon_k)$ of the local Lipschitz condition Assumption 3.3 with respect to the approximate Jacobian $g'(u_k^n)$, and where u_k^* satisfies $r_k(u_k^*) = 0$. Let $\omega_{L,k}$ denote the corresponding Lipschitz constant. Then δ_{k+1} updated by (5.7) with $q_k < 1$, satisfies the following bound with respect to δ_k .

$$\frac{1}{q_k} \left(\delta_k - \frac{\gamma \sigma \omega_{L,k}}{2\|f\|} \|w^n\|^2 \right) \leq \delta_{k+1} \leq \frac{1}{q_k} \left(\delta_k + \frac{\gamma \sigma \omega_{L,k}}{2\|f\|} \|w^n\|^2 \right). \quad (5.11)$$

Proof. Writing δ_{k+1} by the recursive definition given by (5.10), writing out $\mathcal{L}^e(u^n)$ explicitly

$$\delta_{k+1} = \frac{1}{q_k} \left\{ \delta_k + \frac{\gamma \sigma}{\|f\|^2} \langle f, g(u^{n+1}) - g(u^n) - g'(u^n)w^n \rangle \right\}, \quad (5.12)$$

with $u^{n+1} = u^n + w^n$, yielding from the integral mean value theorem

$$g(u^{n+1}) - g(u^n) - g'(u^n)w^n = \int_0^1 (g'(u^n + tw^n) - g'(u^n)) w^n dt. \quad (5.13)$$

Applying a Cauchy-Schwarz inequality to (5.13), and the Lipschitz Assumption 3.3

$$\left\langle f, \int_0^1 (g'(u^n + tw^n) - g'(u^n)) w^n dt \right\rangle \leq \|f\| \frac{\omega_{L,k}}{2} \|w^n\|^2. \quad (5.14)$$

Putting together (5.13) and (5.14) into (5.12) yields the first result, (5.11). This shows where the Lipschitz estimate on Jacobian holds, the variance in δ_{k+1} from a strict reduction by factor q_k is bounded with respect to the Lipschitz constant $\omega_{L,k}$. \square

The next Corollary 5.6 establishes the monotonicity of the sequence $\{\delta_k\}_{k \geq K_0}$ for some finite K_0 , assuming the sequence of residuals $\|r_k\|$ is decreasing. This is imposed by assuming δ is updated on the satisfaction of Criteria 5.1, meaning the iterations converge within the accepted rate on each refinement. An easily imposed lower bound for δ is assumed.

Assumption 5.4. *There is a constant $0 < \delta_{\min} < 1$ for which $0 < \delta_{\min} \leq \delta_k$ for all $k \geq 0$.*

This assumption can be imposed in the definition of δ_{k+1} from δ_k but is given separately for clarity of presentation. The lower bound δ_{\min} is related to generally inaccessible constants which characterize the approximate discrete problems in the next Assumption 5.5. As a guideline, $\delta_{\min} = 1/\gamma_{\max}$ is reasonable as δ tends to increase roughly as $1/\gamma$. A need to impose $\delta > \delta_{\min}$ was not encountered in the numerical experiments presented in Section 7. Along with 5.4, a condition on the data of the approximate problems is assumed, requiring the ratio of $\omega_{L,k}$, the Lipschitz constant for the approximate problem on refinement k , to $\|f_k\|$, remains bounded.

Assumption 5.5. *There is a constant $B_{\omega f}$ for which after some refinement K_1*

$$\frac{\omega_{L,k}}{\|f_k\|} \leq B_{\omega f} \text{ for all } k \geq K_1, \quad (5.15)$$

and the convergence tolerance ε_{CON} of Criteria 5.1 satisfies

$$\varepsilon_{\text{CON}}^2 \leq \frac{\delta_{\min}(1 - q_{\delta}/\bar{q})}{\gamma_k^n \sigma_k^n} \frac{2}{M_{\gamma\sigma}^2} B_{\omega f}^{-1}, \text{ for all } k \geq K_1. \quad (5.16)$$

Corollary 5.6 (Convergence of δ to unity). *Let Assumption 3.5 and the hypotheses of Lemma 5.3 hold. Then δ_{k+1} updated on satisfaction of Criteria 5.1 with $q_k < q_{\delta} < 1$ satisfies $\delta_{k+1} > \delta_k/\bar{q}$ for $q_{\delta} < \bar{q} < 1$ whenever*

$$\delta_k > \frac{\gamma^n \sigma^n}{(1 - q_{\delta}/\bar{q})} \frac{\|r^n\|^2 M_{\gamma\sigma}^2 \omega_{L,k}}{2 \|f_k\|}. \quad (5.17)$$

Additionally, if Assumptions 5.4 and 5.5 hold, then (5.17) holds for all refinements $k > K_0 > K_1$, so long as the residual $\|r_{K_0}\|$ satisfies

$$\|r_{K_0}\|^2 \leq \frac{\delta_{\min}(1 - q_{\delta}/\bar{q})}{\gamma^n \sigma^n} \frac{2}{M_{\gamma\sigma}^2} B_{\omega f}^{-1}, \quad (5.18)$$

and $\delta_k = 1$ for all $k > K$ for some $K \leq \lceil \log(\delta_{K_0})/\log \bar{q} \rceil + K_0$, where $\lceil \cdot \rceil$ denotes the ceiling function.

Proof. Denoting the approximate Jacobian on iteration n by

$$M = (\alpha^n R + \gamma^n (\sigma g'(u^n) + (1 - \sigma)g'(\bar{u}))).$$

In accordance with Assumption 3.5, $\|M^{-1}\| \leq M_{\gamma\sigma}$, and $\|w^n\| \leq \|r^n\| M_{\gamma\sigma}$. Then applying $q_{\delta} > q_k$

$$\frac{\gamma^n \sigma^n}{(1 - q_{\delta}/\bar{q})} \frac{\|r^n\|^2 M_{\gamma\sigma}^2 \omega_{L,k}}{2 \|f_k\|} \geq \frac{\gamma^n \sigma^n}{(1 - q_k/\bar{q})} \frac{\|w^n\|^2 \omega_{L,k}}{2 \|f_k\|}. \quad (5.19)$$

Satisfaction of (5.17) then implies $\delta_k > \delta/\bar{q}$ when δ_k is greater than the quantity on the right of (5.19). Rearranging terms in (5.19) and comparison with (5.11) yields the first result

$$\delta_{k+1} \geq \frac{1}{q_k} \left(\delta_k - \frac{\gamma \sigma \omega_{L,k}}{2 \|f\|} \|w^n\|^2 \right) \geq \frac{1}{\bar{q}} \delta_k. \quad (5.20)$$

Similarly for the second result, $B_{\omega_f}^{-1} < \|f_k\|_{\omega_{L,k}}$, $\delta_{\text{MIN}} < \delta_k$, and for $k \geq K_0$, Criteria 5.1, conditions either (2) or (4) and Assumption 5.5 yield $\|r_k\| \leq \|r_{K_0}\|$, by which satisfaction of (5.18) implies

$$\|r_k\|^2 \leq \frac{\delta_k(1 - q_\delta/\bar{q})}{\gamma^n \sigma^n} \frac{2}{M_{\gamma\sigma}^2} \frac{\|f_k\|}{\omega_{K,L}}. \quad (5.21)$$

Rearranging terms again shows (5.17). So far, this shows $\delta_{k+1} > \delta_k/\bar{q}$ for $k \geq K_0$. A short calculation and Definition 5.2 yield the final result, $\delta_k = 1$ after at most an additional $\lceil \log(\delta_{K_0})/\log \bar{q} \rceil$ refinements and updates of δ . \square

Importantly, the recursive definition (5.10) shows δ is increased more aggressively when the linearization error lies in the direction of f , and is increased less and possibly decreased when $\mathcal{L}^e(u^n)$ is in opposition to f . This sensitivity to direction as opposed to magnitude alone yields added stability to the method. More precisely, the following proposition characterizes the conditions supporting increase of δ in terms of the projection of the linearization error along f . The normalized vector in the direction of f is denoted $\hat{f} = (1/\|f\|)f$.

Proposition 5.7 (Characterization of increase in δ). *The sequence $\{\delta_k\}$ given by the recursive definition (5.10) satisfies $\delta_{k+1} > (1/\bar{q})\delta_k$, $1 < \bar{q} \leq q_k$ whenever*

$$\langle \hat{f}, \mathcal{L}^e(u^n) \rangle > -\delta_k \left(1 - \frac{q_k}{\bar{q}} \right) \frac{\|f\|}{\gamma_k^n \sigma_k^n}. \quad (5.22)$$

The criteria (5.22) follows by direct calculation from (5.10). The lower bound on (5.11) ensures the increase in δ_k in the asymptotic regime as $\|w^n\| \rightarrow 0$ on a given refinement assuring the algorithm eventually converges to the given unscaled data, $\delta = 1$; however, in practice the increase in δ_k is governed by (5.22) through the preasymptotic and coarse mesh regimes.

6. ALGORITHM

The results of the previous sections are summarized in the following algorithm, and combined to yield a proof of convergence using iteration (3.7). The solver using inexact iteration (3.7) is implemented in an adaptive method according to the following basic algorithm. The algorithm using (3.6) is the same, except $\delta = 1$ is assumed throughout.

The additional criteria and parameter settings necessary to define the method are summarized below the algorithm. The choice of parameters to guarantee the monotonic decrease of γ as in Corollary 4.7 is listed as optional. The selection of parameters δ_{MIN} and ε_{CON} to guarantee the monotonic increase in δ as in Corollary 5.6 depend on unknown constants that are not assumed available.

Algorithm 6.1 (Algorithm using the inexact iteration (3.7)). *Set the parameters q_γ , ε_T and γ_{MAX} in accordance with Assumption 4.1 and optionally 4.6. Set the convergence tolerance ε_{CON} and δ_{MIN} of Assumption 5.4. Let $\bar{u} = 0$. Start with initial u^0 , γ^0 , δ_0 . On partition \mathcal{T}_k , $k = 0, 1, 2, \dots$*

- 1) Compute R_k by Definition 3.2, and $g'(\bar{u})$.

- 2) Set $r^0 = -g(u^0) + \delta_0 f_0$, and set $\alpha_0 = \|r^0\|$.
- 3) While Exit criteria 6.2 are not met on iteration $n - 1$:
 - (i) Set σ according to (3.9).
 - (ii) Solve $(\alpha^n R_k + \gamma^n \{\sigma^n g'(u^n) + (1 - \sigma)g'(\bar{u})\})w^n = r^n$, for w^n .
 - (iii) Update $u^{n+1} = u^n + w^n$, and $r^{n+1} = -g(u^{n+1}) + \delta_k f_k$.
 - (iv) If Criteria 4.2 are satisfied, update γ^{n+1} according to Definition 4.3.
 - (v) Update α^n according to (3.4),
- 4) If Criteria 5.1 are satisfied, update δ_{k+1} for partition \mathcal{T}_{k+1} according to (5.2) with $q_\delta = (q_\gamma)^{P+1}$, where P counts the number of times γ was updated on refinement k .
- 5) Compute the error indicators to determine the next mesh refinement.

Criteria 6.2 (Exit criteria). Given a user set tolerance ε_{CON} , and an accepted rate of convergence given by $q_{ACC} = 1 - 1/(2\gamma)$ as in Criteria 5.1, and a baseline number of allowed iterations I_{BASE} , set the maximum number of iterations I_{MAX} by

$$I_{ACC} = \left\lceil \frac{\log(\|r_{k-1}\|) - \log(\|r_k^0\|)}{\log(q_{ACC})} \right\rceil + 1, \quad I_{MAX} = \max\{I_{ACC}, I_{BASE}\}. \quad (6.1)$$

Exit the solver on partition \mathcal{T}_k after calculating residual $\|r^{n+1}\|$ when one of the following conditions holds.

- 1) Condition (5) of Criteria 5.1: the iteration reached convergence.
- 2) Conditions (2-4) of Criteria 5.1: the iteration converges at an acceptable rate and is stopped before convergence.
- 3) Maximum number of iterations I_{MAX} completed: reset γ_{k+1}^0 , δ_{k+1} , and u_{k+1}^0 .

Remark 6.3. Setting the maximum number of iterations by 6.1 prevents a premature exit when the residual is converging close to the predicted rate. An additional failure criteria may be added to exit the iterations quickly if the convergence rate drifts substantially higher than the accepted rate. However, this is mainly useful on very coarse meshes where the problem is small and the linear solves take negligible time.

Remark 6.4 (Initial and reset values for γ , δ , u). An initial set of values for γ , δ , and u are not formally a feature of Algorithm 6.1, however some set of values is required to start the algorithm. The examples shown in Section 7 all use

$$u_0^0 = 0, \quad \gamma_0^0 = \frac{\|f_0\|}{\|g'(u_0^0)\|}, \quad \delta_0 = 1/\gamma_0^0. \quad (6.2)$$

If the iterations fail to converge, i.e., the iterations are terminated on iteration k by condition (3) of Criteria 6.2, u is reset and γ and δ are updated from their previous values by

$$u_{k+1}^0 = 0, \quad \gamma_{k+1}^0 = \min\{2\gamma_k, \gamma_{MAX}\}, \quad \delta_{k+1} = \max\{\delta_k/2, \delta_{MIN}\}. \quad (6.3)$$

Alternatively, γ_{MONO} can take the place of γ_{MAX} in (6.3).

Allowing the possibility of reset is considered an essential part of the algorithm, as the method is designed for capturing steep layers starting from a coarse mesh where the layers may be only partially uncovered or even completely undetected. The approximate discrete problem can drastically change over certain mesh refinements, and the latest update of parameters based on a milder approximate problem may not provide sufficient stability.

The next Assumption 6.5 supposes Algorithm 6.1 resets only finitely-many times, e.g., after some iteration K_A the sequence of problems enters the preasymptotic regime and

iterations on subsequent refinements are terminated by either the first or second condition of Criteria 6.2.

Assumption 6.5. *There exists a refinement K_A , for which either condition (1) or condition (2) of Criteria 6.2 is used to terminate the iterations on refinement k , for all $k \geq K_A$.*

Regardless of whether the exact problem within the target class is well posed, the approximate problems may not be. The coarse mesh problems are often ill-posed, may feature indefinite and ill-conditioned Jacobians, and there is no guarantee that even an exact solution to a given approximate problem will land in any basin of attraction for the approximate problem on the subsequent refinement.

An analysis of the problem class where Algorithm 6.1 can be proven to converge, *i.e.*, where Assumption 6.5 can be shown to hold, is beyond the scope of the current paper. The numerical examples in the next section demonstrate the performance of the algorithm on a range of problems with steep internal and boundary layers, as well as highly variable solution dependent frequencies in the diffusion coefficient. The following Theorem 6.6 summarizes the theoretical convergence properties of Algorithm 6.1 within the problem class characterized by Assumption 6.5.

Theorem 6.6. *Assume the hypothesis of Corollary 4.7 and Corollary 5.6, and let Assumption 6.5 hold for $k \geq K_A$. Then the iterations on refinements $k \geq K_B$ for $K_B \leq K_A + N_A + N_B$ with N_A and N_B given by (6.4) and (6.5), attain convergence up to tolerance ε_{CON} with $\delta = 1$. Further assuming the hypotheses of Theorem 3.6, there is a refinement K_C for which $\gamma_k = 1$ for $k \geq K_C$.*

The convergence of γ to one is not necessary for the convergence of the iterations, but it is necessary for its efficiency, and the asymptotically quadratic convergence of the resulting iterations as discussed in [2, 18, 22, 21].

Proof. The convergence of the sequence of residuals $\|r_k\| \rightarrow 0$ within tolerance ε_{CON} follows directly from Criteria 5.1. Assuming $\|r_{K_A}\| > \varepsilon_{\text{CON}}$ and $\gamma \leq \gamma_{\text{MONO}}$ from Assumption 4.6, direct calculation shows after at most N_A refinements, the iterations achieve convergence of the residual, with N_A given by

$$N_A = \left\lceil \frac{\log(\varepsilon_{\text{CON}}/\|r_{K_0}\|)}{\log(1 - 1/2\gamma_{\text{MONO}})} \right\rceil. \quad (6.4)$$

In particular, $\|r_k\| < \varepsilon_{\text{CON}}$ for $k \geq K_B = K_A + N_A$. From Corollary 5.6 and Assumption 5.5, it also holds if $\delta_{K_B} < 1$, the sequence $\delta_k, k \geq K_B$ increases monotonically to unity, and for $q_\gamma < \bar{q} < 1$ it follows that $\delta_k = 1$ for $k \geq K_C = K_B + N_B$, with

$$N_B = \lceil \log \delta_{K_B} / \log \bar{q} \rceil. \quad (6.5)$$

This establishes the first result, the convergence of the sequence of residuals to zero for the problem defined with consistent data.

The second part of the argument demonstrates the decrease of γ to 1 follows from the local convergence Theorem 3.6. Assuming the residual is small enough, then the rate $\|r^{n+1}\|/\|r^n\|$ asymptotically approaches $1 - 1/\gamma$, and in particular is within ε_T tolerance of the predicted rate, meaning Criteria 4.2 hold, and γ is updated by Definition 4.3; and, by Corollary 4.7 converges to one after at most an additional $N_C = \lceil -\log(\gamma_{\text{MONO}})/\log \bar{q} \rceil$ updates. The subtle point is the convergence tolerance ε_{CON} must be small enough for the asymptotic convergence rate of Theorem 3.6 to be assured. \square

Remark 6.7. *It is not just an artifact of the analysis that $\gamma \rightarrow 1$ cannot be assured until after the iterations already achieve convergence to tolerance on every iteration, and*

that the tolerance ε_{CON} must be sufficiently small. The phenomenon of γ stalling above one and failing to update for several iterations after $\|r_k\| < \varepsilon_{\text{CON}}$ has been observed, in particular in problems similar to Example 7.2 in the next section, where a diffusion coefficient with a high frequency dependence on the solution fails to resolve until the mesh in the highest-frequency region is sufficiently fine. It is more commonly observed that the iterations do converge at the predicted rate when the residual is far from convergence, but generally $\gamma \rightarrow 1$ within a few iterations on either side of the residual converging to tolerance.

7. NUMERICAL EXAMPLES

The numerical experiments were performed with a Python implementation of the FEniCS library [19], and additional Numpy [17] computations. For each of the examples shown, Algorithm 6.1 is demonstrated solving for both a known and an unknown solution. The unknown solution examples demonstrate the effectiveness of the method for cases where the variable dependent and solution dependent layers may not match up. For the source functions designed to produce a known solution, the H^1 and L_2 errors denoted by $|u - u_k|_1$ and $|u - u_k|_0$, respectively, are shown along with the error estimator; otherwise, the error estimator is shown to decay at the expected rate of $n^{-1/2}$ for degrees of freedom n , after the resolution of the layers.

The examples are all run with reduction factor $q_\gamma = 0.9$ and $\sigma_0 = 0.9$. The Dörfler parameter of (3.3) is set to $\theta = 0.2$, at the tolerance $\varepsilon_{\text{CON}} = 10^{-7}$. Example 7.2 with the unknown source (7.8) uses rate tolerance $\varepsilon_T = 0.01$, and all other examples use $\varepsilon_T = 0.005$. The higher rate tolerance is used to prevent the update of γ from stalling in cases where a high mesh resolution is necessary to accurately capture the Jacobian. Perturbing these parameter settings may change the number of refinements or the number of resets taken for the algorithm to arrive at the asymptotic regime, but not the end result. The initial and reset values of u , γ , and δ are set as in Remark 6.4 in accordance with Assumption 4.2 but not necessarily Assumption 4.6. Nonetheless, monotonicity of the parameters is generally observed on iterations when the algorithm does not reset. Each example is started on a uniform mesh of 144 triangular elements.

Example 7.1 (Steep internal layer). *Consider the quasilinear diffusion equation on $\Omega = [0, 1] \times [0, 1]$.*

$$F(u, x) := -\text{div}(\kappa(u)\nabla u) - f(x, y) = 0 \text{ in } \Omega, \quad u = 0 \text{ on } \partial\Omega. \quad (7.1)$$

The solution dependent diffusion coefficient is given by

$$\kappa(s) = k + \frac{1}{\varepsilon + (s - a)^2}, \quad \text{with } a = 0.5, \quad k = 1, \quad \text{and } \varepsilon = 6 \times 10^{-5}. \quad (7.2)$$

The following source functions are considered

$$f(x, y) \text{ chosen so } u(x, y) = \sin(\pi x) \sin(\pi y), \quad (7.3)$$

$$f(x, y) = 10^5 \cdot (0.5 - |x - 0.5|)^2 (0.5 - |y - 0.5|). \quad (7.4)$$

The diffusion coefficient $\kappa(s)$ is bounded away from zero with $\kappa(s)$, $\kappa'(s)$ and $\kappa''(s)$ all bounded assuring uniqueness of the solution as in [4]. Milder versions of this model problem with source (7.3) are considered by the author in [22, 21]. The inexact iteration (3.7) allows the solver to stabilize on a coarser mesh and with steeper gradients in the diffusion term than in previous versions of the method. Figure 1 on the left shows an adaptive mesh in the preasymptotic regime for Example 7.1 with source (7.3) showing local refinement of the internal layer with the mesh remaining coarse away from the layer.

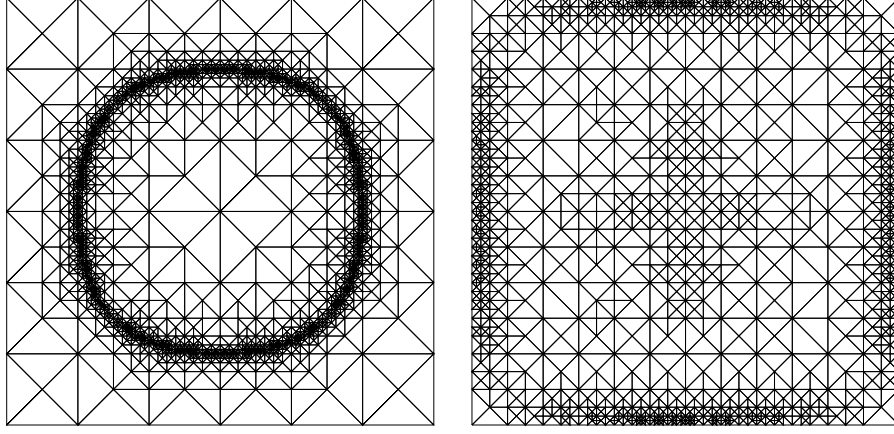


FIGURE 1. Adaptive meshes from Example 7.1. Left: mesh after 20 iterations with 4140 elements for source (7.3). Right: mesh after 25 iterations with 2208 elements for source (7.4).

The mesh on the right shows the boundary and internal layer resolution for Example 7.1 with source (7.4).

Figure 2 shows the H^1 error, the L_2 error and the error estimator running from the course mesh regime through the preasymptotic and into asymptotic regime. The transition from the coarse mesh to preasymptotic is captured by the increase in error within the first twelve iterations, and through the nonmonotonicity of parameters γ and δ , shown on the right. The decreases in δ , and the corresponding increases in γ during this phase are due to reset of the algorithm. The transition from the preasymptotic to the asymptotic regime is displayed as a sharp decrease in L_2 error and the estimator η as δ approaches one and the iteration solves for a right hand side consistent with the problem data. This sharp drop can be smoothed over several iterations by allowing a few preliminary refinements based only on the variable dependent data or otherwise stalling the initial increase of δ , but these techniques were not used in the current work in order to better illustrate the range of possible behaviors of the inexact method. In the plot of the parameters γ and δ , Figure 2 also illustrates how the initial relationship $\gamma = 1/\delta$ is approximately maintained when the iterations maintain stability through the mesh refinements.

Figure 3 shows the behavior of the error estimator next to a plot of the parameters γ and δ for the diffusion problem of Example 7.1 with a nonsmooth source (7.4). The initial coarse mesh problem is a bad representation of the exact problem resulting in early resets of the algorithm, after which enough of the data is captured to maintain stability through the mesh refinements. In contrast to the same diffusion operator with source (7.3), here the error estimator grows throughout the preasymptotic regime as δ increases to one, then decreases at the predicted rate of $n^{-1/2}$ with respect to degrees of freedom n .

Example 7.2 (Oscillatory diffusion with several layers). *Consider the quasilinear diffusion equation on $\Omega = [0, 1] \times [0, 1]$.*

$$F(u, x) := -\operatorname{div}(\kappa(u)\nabla u) - f(x, y) = 0 \text{ in } \Omega, \quad u = 0 \text{ on } \partial\Omega. \quad (7.5)$$

The solution dependent diffusion is given by

$$\kappa(s) = k + \sin(s/\varepsilon) + \arctan(s/\varepsilon), \quad \text{with } \varepsilon = 6 \times 10^{-3}. \quad (7.6)$$

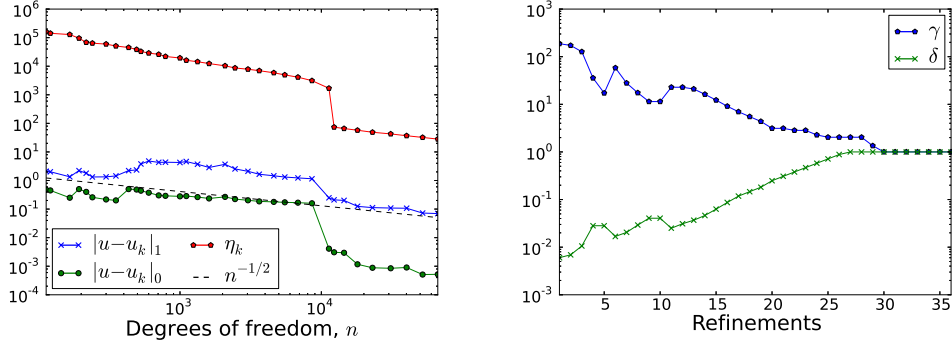


FIGURE 2. Left: H^1 error, L_2 error, and error estimator (above) against $n^{-1/2}$ where n is the number of degrees of freedom. Right: parameters γ and δ for Example 7.1 with source (7.3).

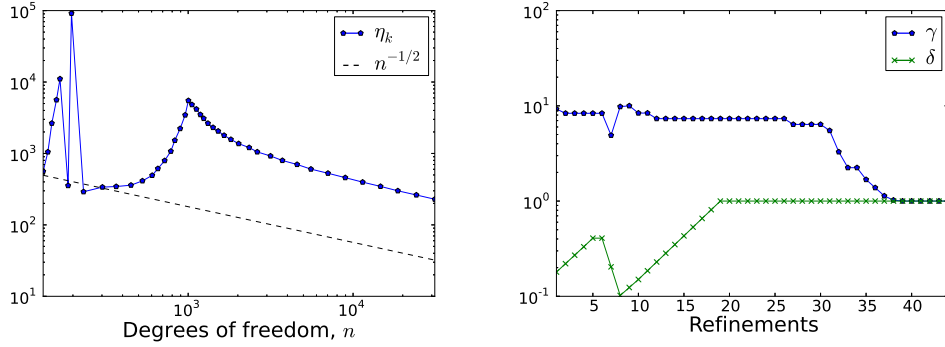


FIGURE 3. Left: Error estimator η against $n^{-1/2}$ where n is the number of degrees of freedom. Right: parameters γ and δ for Example 7.1 with source (7.4).

The following source functions are considered, with the k from (7.6) set to $k = 2 + \pi/2$ with source (7.7) and $k = 10$ with source (7.8).

$$f(x, y) \text{ chosen so } u(x, y) = 1.85^4 \cdot x(x-1)y(y-1) - 2^8 \cdot x^{9/4}(x-1)^2y^2(y-1)^2, \quad (7.7)$$

$$f(x, y) = (1-x)(1-y)(e^{8x^2} - 1)(e^{8y^2} - 1). \quad (7.8)$$

By the same reasoning as Example 7.1, this problem has a unique solution. Example 7.2 demonstrates the inexact method on a problem where in addition to steep gradients, the diffusion coefficient features oscillations proportional in frequency to the magnitude of solution u . Similar to the first example the error decreases throughout all iterations with minor fluctuations for the source with the known solution (7.7). In this case for the source corresponding to an unknown solution (7.8), the estimator first decreases then stabilizes and increases as δ increases to one, and then decreases at a steady rate.

For both source functions in Example 7.2, the decrease in γ stalls for several iterations in the preasymptotic regime. This shows the iterations are not converging at the expected rate for several refinements, presumably because the solution-dependent frequencies of the diffusion coefficient $\kappa(u)$, are not sufficiently well expressed on the mesh as the solution u first attains a threshold frequency.

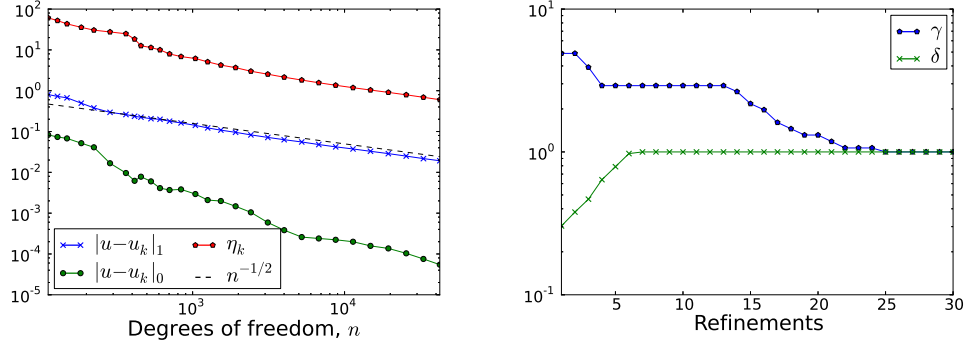


FIGURE 4. Left: H^1 error, L_2 error and error estimator (above) against $n^{-1/2}$ where n is the number of degrees of freedom. Right: parameters γ and δ for Example 7.2 with source (7.7).

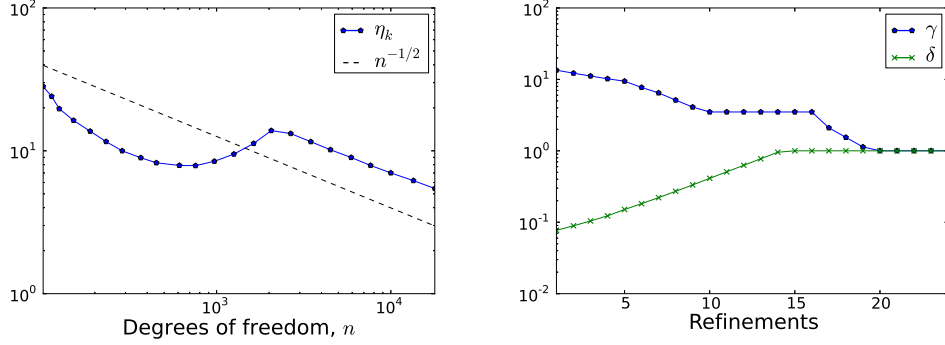


FIGURE 5. Left: Error estimator against $n^{-1/2}$ where n is the number of degrees of freedom. Right: parameters γ and δ for Example 7.2 with source (7.8).

Example 7.3 (Gradient-dependent diffusion coefficient). *Consider the quasilinear diffusion equation on $\Omega = [0, 1] \times [0, 1]$.*

$$F(u, x) := -\operatorname{div}(\kappa(|\nabla u|^2)\nabla u) - f(x, y) = 0 \text{ in } \Omega, \quad u = 0 \text{ on } \partial\Omega. \quad (7.9)$$

The solution dependent diffusion coefficient is given by

$$\kappa(t^2) = k + \arctan((t^2 - a)/\varepsilon), \quad \text{with } a = \pi, \quad k = \pi, \quad \text{and } \varepsilon = 2 \times 10^{-2}. \quad (7.10)$$

The following source functions are considered

$$f(x, y) \text{ chosen so } u(x, y) = \sin(\pi x) \sin(\pi y), \quad (7.11)$$

$$f(x, y) = 2 \times 10^3 \cdot (0.5 - |x - 0.5|)^2 (0.5 - |y - 0.5|)^2. \quad (7.12)$$

As in [14], monotonicity and Lipschitz conditions are established by observing there are positive constants c and C with $c \leq \kappa(t^2) + 2t^2\kappa'(t^2) \leq C$, assuring a unique solution to the exact problem. This is not known for the approximate problems, particularly on the coarse meshes. This example with source (7.11) illustrates the phenomenon of multiple resets as thin layers in both the source $f(x)$ and the Jacobian are uncovered. Figure 6 corresponding to Example 7.3 with source (7.11) shows several jumps up in the error corresponding to the resets, a steep decrease as $\delta \rightarrow 1$ and the discrete problem regains consistency, then steady decrease in the error at the predicted rate. The plot on the right shows γ stalling for several refinements after the last reset until the approximate

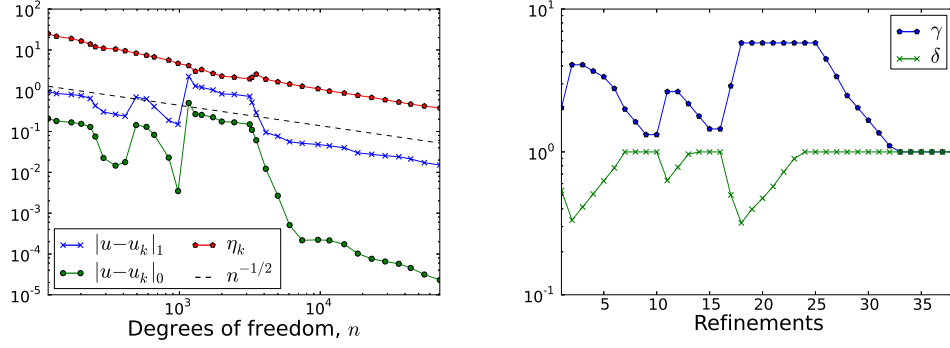


FIGURE 6. Left: H^1 error, L_2 error and error estimator (above) against $n^{-1/2}$ where n is the number of degrees of freedom. Right: parameters γ and δ for Example 7.3 with source (7.11).

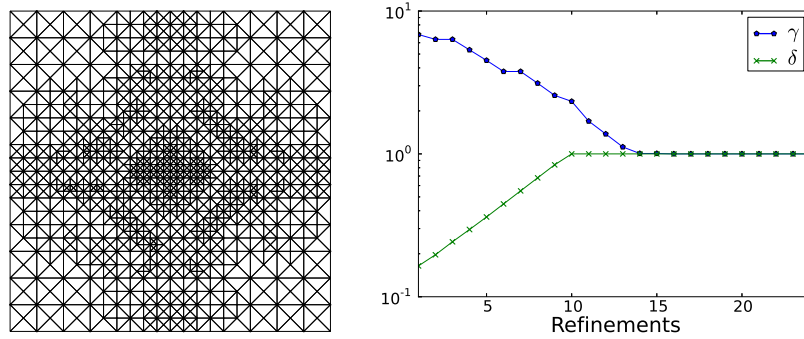


FIGURE 7. Left: adaptive mesh from Example 7.3 with source (7.12) after 12 refinements with 1914 elements. Right: parameters γ and δ .

Jacobian is sufficiently well resolved and Criteria 4.2 for updating γ are met before Criteria 5.1 determines the iterations should stop. Once necessary resolution is achieved, γ reduces quickly to one and the residual is solved to tolerance within a few iterations on subsequent refinements.

The decrease in the estimator is relatively steady in comparison to the H^1 error, and does not indicate that preliminary to the resets the correction steps w^n fail to update the solution u^n to sufficiently decrease the residual $\|r^n\|$. In this case the update steps w^n display a loss of stability due to a qualitative change in the problem data from the latest mesh refinement, albeit at a magnitude small in comparison to u^n , and the reset is performed before the solution is dominated by unstable fluctuations.

For source (7.12) corresponding to the unknown solution, the estimator decreases similarly to the one for source (7.11). The adaptive mesh for the twelfth refinement, just as $\gamma \rightarrow 1$ is shown on the left of Figure 7, next to a plot of parameters γ and δ . The mesh shows the most dense refinement in the center, corresponding to the peak of the source, with additional refinement along the discontinuities of its gradient. Additional dense refinement is seen developing along the steep gradients of $\kappa(|\nabla u|^2)$.

8. CONCLUSION

An updated adaptive method for the numerical solution of quasilinear diffusion problems with steep internal layers is presented, building on the previous work by the author

in [22, 21]. The goal of this method is to start the computation on a coarse mesh where the solution and variable dependent problem coefficients are not resolved, and to partially solve the possibly ill-posed approximate coarse mesh problems up to sufficient tolerance to refine the mesh and eventually achieve a stable and efficient computation of the solution to an accurate representation of the problem. The current results include explicit definitions for the added numerical dissipation parameter γ used to stabilize the iterations on the coarse mesh, and the introduction of an inexact method to further stabilize problems where the residual is dominated by a variable dependent source. The scaling parameter δ of the inexact method is shown to reach one which demonstrates consistency of the method, and the convergence of the residual of the discrete nonlinear problem is established. Under convergence of the residual, the parameter γ is also shown to reach one, establishing efficiency of the Newton-like iterations in the asymptotic regime. Future work by the author will include adapting the current method for quasilinear convection problems and nonhomogeneous boundary conditions, as well as investigation of the stabilization properties of inexact linear solves.

REFERENCES

- [1] G. AWANOU, *Standard finite elements for the numerical resolution of the elliptic Monge-Ampère equation: classical solutions*, IMA Journal of Numerical Analysis, (2014).
- [2] R.E. BANK AND D.J. ROSE, *Parameter selection for Newton-like methods applicable to nonlinear partial differential equations*, SIAM J. Numer. Anal., 17 (1980), pp. 806–822.
- [3] L. BELENKI, L. DIENING, AND C. KREUZER, *Optimality of an adaptive finite element method for the p -Laplacian equation*, IMA J. Numer. Anal., 32 (2012), pp. 484–510.
- [4] G. CALOZ AND J. RAPPAZ, *Numerical analysis for nonlinear and bifurcation problems*, Handbook of Numerical Analysis, (1994).
- [5] G. CHEN, J. ZHOU, AND W.-M. NI, *Algorithms and visualization for solutions of nonlinear elliptic equations*, Internat. J. Bifur. Chaos. Appl. Sci. Engrg., 10 (2000), pp. 1565–2612.
- [6] J. CHUNG AND G. M. HULBERT, *A time integration algorithm for structural dynamics with improved numerical dissipation: The generalized- α method*, J. Appl. Mech., 60 (1993), pp. 371–375.
- [7] P. G. CIARLET, *Finite Element Method for Elliptic Problems*, Society for Industrial and Applied Mathematics, Philadelphia, PA, USA, 2002.
- [8] T. S. COFFEY, C. T. KELLEY, AND D. E. KEYES, *Pseudo-transient continuation and differential-algebraic equations*, SIAM J. Sci. Comput., 25 (2003), pp. 553–569.
- [9] L. EL ALAOU, A. ERN, AND M. VOHRALK, *Guaranteed and robust a posteriori error estimates and balancing discretization and linearization errors for monotone nonlinear problems.*, Computer Methods in Applied Mechanics and Engineering, 200 (2011), pp. 2782 – 2795.
- [10] H.W. ENGL, M. HANKE, AND A. NEUBAUER, *Regularization of Inverse Problems*, Mathematics and Its Applications, Springer, 1996.
- [11] A. ERN AND M. VOHRALK, *Adaptive inexact Newton methods with a posteriori stopping criteria for nonlinear diffusion PDEs*, SIAM J. Sci. Comput., 35 (2013), pp. A1761–A1791.
- [12] F. FIERRO AND A. VEESER, *On the a posteriori error analysis for equations of prescribed mean curvature*, Math. Comput., 72 (2003), pp. 1611–1634.
- [13] K. FOWLER AND C.T. KELLEY, *Pseudo-transient continuation for nonsmooth nonlinear equations*, SIAM J. Numer. Anal., 43 (2005), pp. 1385–1406.
- [14] E. M. GARAU, P. MORIN, AND C. ZUPPA, *Convergence of an adaptive Kačanov FEM for quasilinear problems*, Applied Numerical Mathematics, 61 (2011), pp. 512 – 529.
- [15] H. M. HILBER AND T. J. R. HUGHES, *Collocation, dissipation and overshoot for time integration schemes in structural dynamics*, Earthquake Eng. Struc., 6 (1978), pp. 99–117.
- [16] M. HOLST, G. TSOGTGEREL, AND Y. ZHU, *Local and global convergence of adaptive methods for nonlinear partial differential equations*, 2008.
- [17] E. JONES, T. OLIPHANT, P. PETERSON, ET AL., *SciPy: Open source scientific tools for Python*, 2001–.
- [18] C. T. KELLEY AND D. KEYES, *Convergence analysis of pseudo-transient continuation*, SIAM J. Numer. Anal., 35 (1998), pp. 508–523.

- [19] A. LOGG, K-A. MARDAL, G. N. WELLS, ET AL., *Automated Solution of Differential Equations by the Finite Element Method*, Springer, 2012.
- [20] N. M. NEWMARK, *A method of computation for structural dynamics*, J. Eng. Mech.-ASCE, 85 (1959), pp. 67–94.
- [21] S. POLLOCK, *An improved method for solving quasilinear convection diffusion problems*, 2015. Available as arXiv:1502.02629 [math.NA].
- [22] ———, *A regularized Newton-like method for nonlinear PDE*, Numer. Func. Anal. Opt., 36 (2015), pp. 1493–1511.
- [23] R. STEVENSON, *Optimality of a standard adaptive finite element method*, Found. Comput. Math., 7 (2007), pp. 245–269.
- [24] J. XU, *Two-grid discretization techniques for linear and nonlinear PDEs*, SIAM J. Numer. Anal., 33 (1996), pp. 1759–1777.

E-mail address: snpolloc@math.tamu.edu

DEPARTMENT OF MATHEMATICS, TEXAS A&M UNIVERSITY, COLLEGE STATION, TX 77843